Differential behavior of pericytes and adipose stromal cells in vasculogenesis and angiogenesis

Julian Gonzalez-Rubio[1], Hiltrud Königs-Werner[2], Christian G. Cornelissen[1, 3], Anja Lena Thiebes[1]

[1] Department of Biohybrid & Medical Textiles (BioTex), AME - Institute of Applied Medical Engineering, Helmholtz Institute, RWTH Aachen University, Germany

[2] Institute of Pathology, Electron Microscopy Facility, RWTH Aachen University Hospital, Aachen, Germany

[3] Clinic for Pneumology and Internal Intensive Care Medicine (Medical Clinic V), RWTH Aachen University Hospital

Abstract

Perfusable vascularization of tissue-engineered systems remains one of the main hurdles in producing large-scale functional tissues. Blood vessel formation by endothelial cells is dependent on supporting cells such as stromal cells. From them, the pericyte is the most relevant due to its close interaction with the endothelial cells, protecting them from external harm and architecting new vessels and connections. However, the identity of this cell type and its relation with other mesodermic cells, such as the mesenchymal stromal/stem cells, is highly debated. In this study, we delve into the distinct behavior of stromal cells and pericytes in the context of vascularization. The protein MCAM/CD146 was proposed as a specific marker for pericyte selection from adipose-derived stromal cells. By employing microfluidic chips that consist of an internal chamber flanked by two parallel media channels, we replicated the primary processes involved in vessel formation: vasculogenesis, which refers to the de novo vessel formation, and angiogenesis, the sprouting of new vessels from existing ones. In angiogenesis, pericytes promoted significantly more and bigger sproutings than the stromal cells. In vasculogenesis, stromal cells promoted the formation and proliferation of endothelial structures similar to the embryonic capillary plexus, whereas pericytes arrested the endothelial cell division and forced them to form vessel-like structures. Furthermore, pericytes exhibited an intimate interaction with endothelial cells leading to the synthesis of a shared basement membrane between these cell types, which was rarely observed for its unselected counterpart. Bulk mRNA sequencing confirmed an upregulation of pro-vascularization and cytostatic genes in co-cultures of pericytes and endothelial cells; while stromal cells strongly stimulate mitosis and organelle biogenesis pathways, and decrease inflammatory cytokines, explaining the different vasculogenesis outcomes. We therefore confirm MCAM as a specific marker for pericyte isolation from adipose tissue, also showing that this cell type acts as a mural cell in co-culture with endothelial cells in microfluidic chips, promoting their angiogenic sprouting and vasculogenic tubulogenesis.

Introduction

The circulatory system is the interconnected and hierarchical network of vessels that irrigate most human tissues, nourishing the cells with nutrients and oxygen, removing waste products, and serving as a connection for the endocrine and immune systems to swiftly reach any part of the body (Yang et al. 2020). All vessels are lined with endothelial cells. In the capillaries, the smallest branch of the circulation, endothelial cells are lined externally by a mural cell type known as pericyte, which supports

its homeostasis, protects it from stromal debris by phagocytosis and regulates the blood flow (Zhao and Chappell 2019).

For tissue engineering, the size of avascularized bioengineered organs is limited to a few hundred micrometers (Chandra and Atala 2019). Any thicker tissue will eventually lead to cell death without irrigation of a blood-mimicking fluid due to the lack of oxygen and nutrient diffusion to the innermost cells, causing the formation of a necrotic core. However, achieving vascularization in *in vitro* systems is still a challenge due to the complexity of the process and the variety of cells involved (Zhang and Radisic 2020).

Human adipose tissue is an easily obtainable biological source, which can be digested using collagenases to extract a heterogeneous mixture of cells, known as stromal vascular fraction (SVF) (Sun et al. 2019). The spindle-shaped cells produced by seeding the SVF on cell culture-treated plastic are often referred as adipose-derived mesenchymal stromal/stem cells or adipose stromal cells, from now on termed in this study just as stromal cells (Bourin et al. 2013). They have been widely reported to have immunomodulatory properties (Melief et al. 2013) and *in vitro* multipotency (Brooks et al. 2019). Within this heterogeneous collection, we can find a wide variety of stromal cells such as fibroblasts, pre-adipocytes, and the previously mentioned pericytes (Sun et al. 2019). The Melanoma Cell Adhesion Molecule (MCAM), also known as Cluster of Differentiation (CD) 146, can act as a mural cell marker for bone marrow-derived stromal cells (Blocki et al. 2013) and has been proposed as a specific membrane protein for adipose-resident pericyte isolation (Wang et al. 2019). Importantly, MCAM is not exclusive to pericytes and can be expressed in other vascular-related cell types such as lymphocytes and endothelial cells, but these cells can be depleted due to their incapability or inefficiency to attach and divide on uncoated hydrophilic plastic surfaces (Wang et al. 2020). The identity of pericytes *in vivo* and, especially, *in vitro*, are however widely debated (Caplan 2017; Blocki et al. 2013). So is their relationship with mesenchymal stem cells, their contribution to vascularization processes, and their use in cell therapies and tissue engineering (Blocki et al. 2018; Kosyakova et al. 2020; Zhao and Chappell 2019; Souza et al. 2016; Guimarães-Camboa et al. 2017).

In recent years, microfluidic devices have allowed the creation of organ-on-chip technologies, also known as microphysiological systems (Leung et al. 2022). These platforms have been demonstrated as powerful tools for the study of tissue development, cell-cell and cell-matrix interaction, and vascularization (Vila Cuenca et al. 2021; Alimperti et al. 2017). Here, we use a microfluidic platform to mimic vasculogenic and angiogenic processes, comparing how pericytes and stromal cells interact with endothelial cells to form the vessels and promote their growth. The present study is based on two hypotheses, (1) that CD146 serves as a reliable marker for the selection of pericytes from heterogenous adipose stromal cells, and (2) that pericytes can be cultured *in vitro* without losing the capacity to act as mural cells, promoting more vessel formation than their unselected counterpart, ensheating themselves and the associated endothelial cells into a shared basement membrane.

Results and discussion

Microfluidic chips as a platform for the study of vessel formation through vasculogenesis and angiogenesis

Vascularization can be achieved by vasculogenesis, in which ECs organize themselves into interconnected vessels, or by angiogenesis, where new vessels originate from pre-existing ones (Figure 1A). To compare both mechanisms and how pericytes and stromal cells act in both of them, we used a three-channel microfluidic chip (Figure B). For mimicking vasculogenesis, both the ECs and the supporting cells are added into the hydrogel in the middle chamber, while for the angiogenesis only

the supporting cells are added in the middle chamber and one of the channels is coated with ECs (Figure C). The pre-staining of the cells with lipophilic dyes confirms the deposition of the cells after gel injection. Imaging of the chips 24 hours after the preparation shows the endothelial cells attached to the hydrogel-media interface in the angiogenesis condition, marking the beginning of angiogenesis (Figure C, right image).

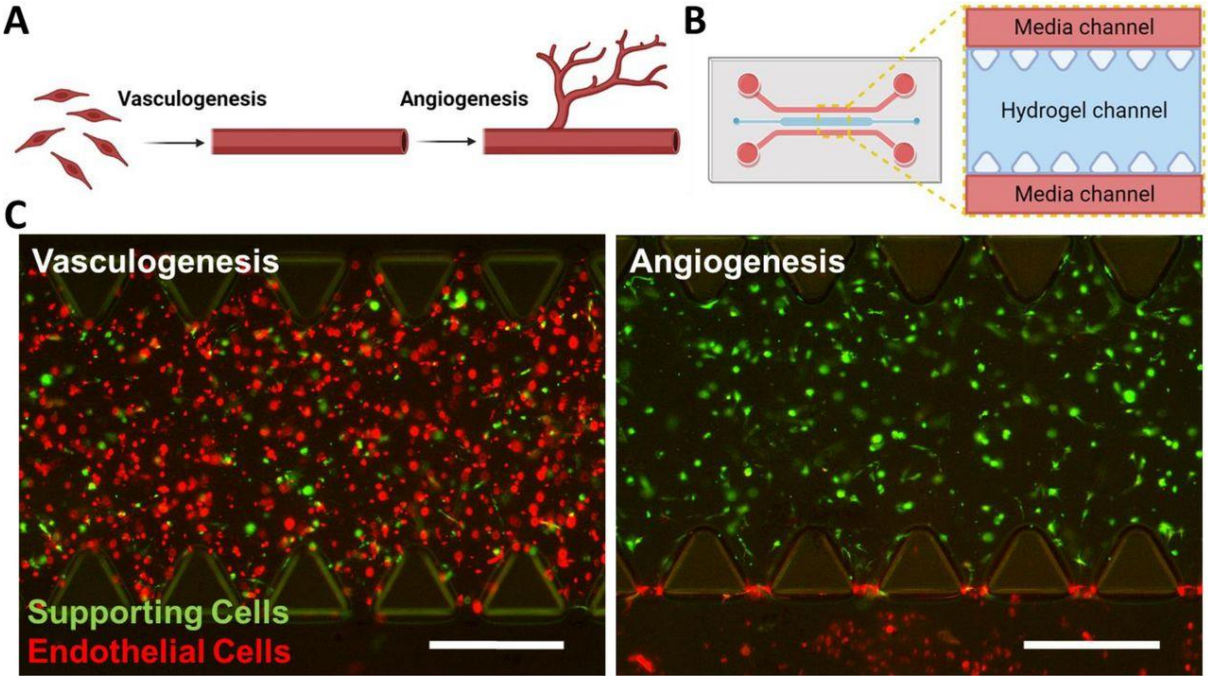

Figure 1. Replication of the two main neovascularization processes in microfluidic devices

(A) Main mechanisms of vessel formation in the human body.

(B) Schematic drawing showing the internal hydrogel chamber (blue) and the surrounding parallel media channels (red).

(C) Fluorescence image showing endothelial cells (Vybrant DiD, red) and supporting cells (Vybrant DiO, green), which can be either pericytes or stromal cells, in two different set-ups to study vasculogenesis and angiogenesis. Scale bars: 500 µm.

MCAM-enriched stromal cells act as pericytes in vitro and show enhanced pro-angiogenic potential

We separated pericytes from the heterogenous adipose SVF based on the expression of the mural cell marker MCAM/CD146 using immunomagnetic microbeads. Both pericytes and normal unselected stromal cells were cultured in mesenchymal cell culture media and expanded. To investigate how these cell types compare to each other in promoting vascularization, three donors of each cell type were co-cultured with endothelial cells in microfluidic devices, as previously described in the angiogenesis setup (Figure 1C, right). The co-cultures were maintained for ten days, fixed and stained for the endothelial marker CD31, and for F-actin to mark the supporting cells.

Imaging of the devices shows that pericytes are promoting more vessel sprouting than the stromal cells (Figures 2A-F). Statistically significant differences can be found in both the vessel volume and branching points (Figures 2C and F). Pericytes have been already reported to be highly pro-angiogenic supporting cells due to their close relation with ECs *in vivo* (Kosyakova et al. 2020; Blocki et al. 2013; Yamazaki and Mukouyama 2018). Although differences can be also observed between the length and area of the sproutings, these are not statistically significant due to the considerable donor-to-donor

variability (Figure 2B and D). Interestingly, these results are not correlated with any remarkable difference in vessel diameter (Figure 2E).

As can also be observed in the augmented immunofluorescence image, the pericytes tend to be significantly closer or even directly associated with the vessels, while the stromal cells remain homogenously distributed in the gel (Figures 2A and G). This interaction is expected from pericytes, which are known to wrap around blood vessels *in vivo* to support and regulate their functions (Yamazaki and Mukouyama 2018).

A bead-based immunoassay for flow cytometry was used to measure and compare the concentrations of eleven proteins highly related to angiogenesis in the cell media collected on the last day of culture (Figure 2H). Despite the strong differences in performance between both supporting cell types, no significant difference was found. However, cell-cell communication during angiogenesis is not reduced to free biomolecules in the environment. Exosomes, lipidic vesicles loaded with biomolecules that are released and fused with other cells, have been consistently related to pro-angiogenic mechanisms in both pericytes and stromal cells (Todorova et al. 2017). Also, as previously shown, pericytes have close contact with the vessels, allowing a direct cell-cell pro-angiogenic stimulation without the need for growth factor release into the media (Caporali et al. 2017; Sweeney and Foldes 2018). We can therefore confirm that the MCAM-selected pericytes maintain their pro-angiogenic activity and mural cell behaviour *in vitro*.

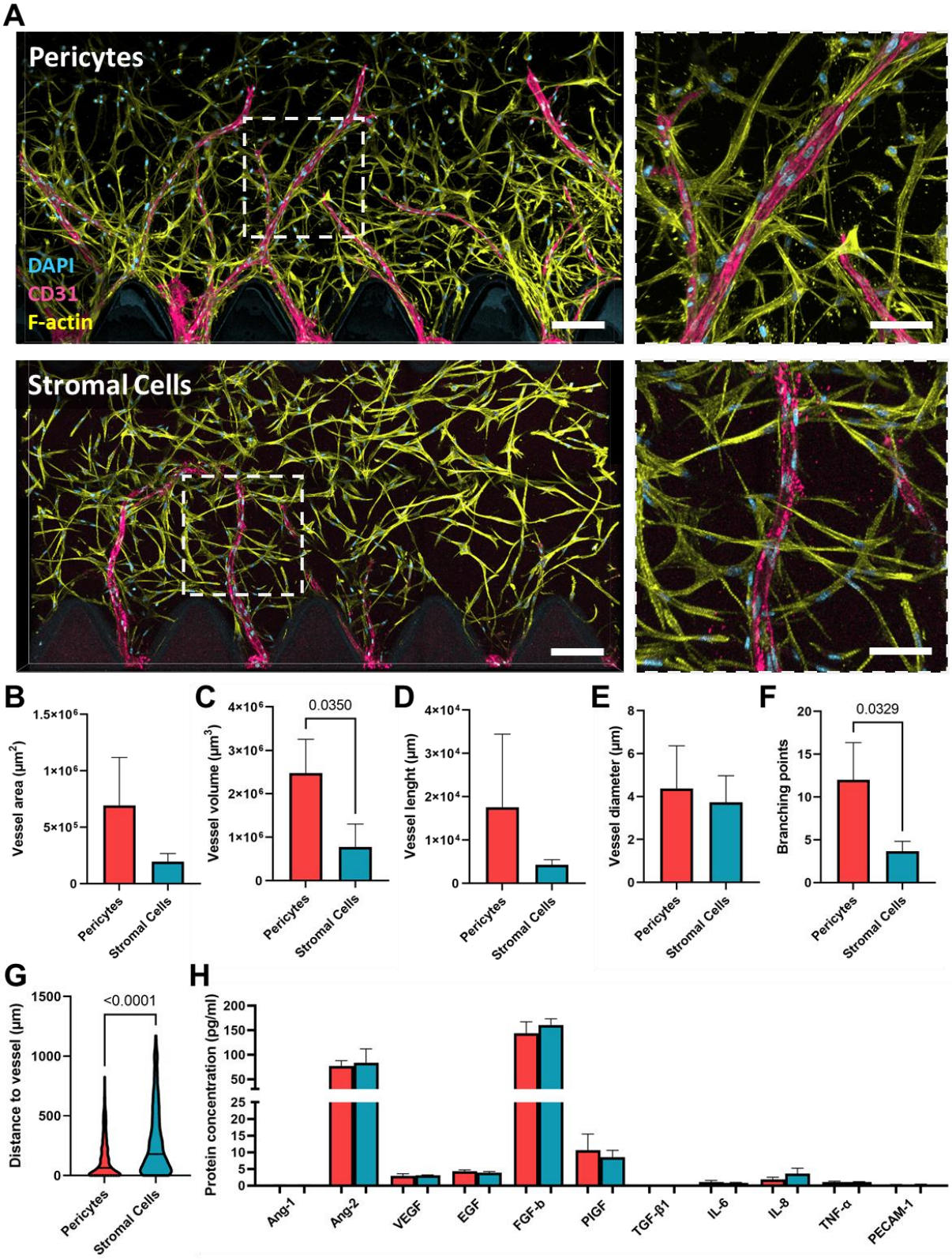

Figure 2. Comparison of the pro-angiogenic potential of pericytes and stromal cells.

(A) Immunofluorescence images of the angiogenic sprouting within the microfluidic chips co-cultured with either pericytes or stromal cells, stained for nuclei (DAPI; cyan), CD31 showing the endothelial vessel-like structures (magenta) and the supporting cells actin cytoskeleton (Phalloidin; yellow). F-actin is not visible within the endothelial cells since it was subtracted from the picture during the image processing to increase clarity. Scale bar: 200 µm (left), 100 µm (right).

(B-F) Comparison of vessels' total area, volume, length, average diameter, and branching points between both co-culture conditions (n = 3, t-test).

(G) Comparison of the distance between each type of supporting cell and the nearest vessel-like structure. The trunked violin plots depict summary statistics and the kernel density estimation to show the frequency distribution of each condition. The middle line represents the median (n = 3, Mann-Whitney test).

(H) Quantification of vascular-related proteins present in the cell culture media after 10 days of culture. Protein names: Angiopoietins 1 and 2 (Ang-1/-2), Vascular Endothelial Growth Factor (VEGF), Epidermal Growth Factor (EGF), Fibroblast Growth Factor-basic (FGF-b), Placental Growth Factor (PlGF), Tumor Growth Factor-beta 1 (TGF-β1) interleukins 6 and 8 (IL-6/-8), Tumor Necrosis Factor-alpha (TNF-α) and Platelet endothelial cell adhesion molecule (PECAM-1) (n = 3, t-test; corrected for multiple comparisons).

Pericytes promote vessel formation during vasculogenesis, while stromal cells stimulate endothelial cell proliferation

Immunofluorescence images of the microfluidic device comparing pericytes and the unselected stromal cells in vasculogenesis (Figure 1C, left) show clear differences between how both cell types support endothelial cell coalescence and elongation (Figure 3A). Pericytes promote the formation of long and thin tubular endothelial structures, while co-culture with stromal cells leads to the formation of bloated and amorphous structures. Quantification of the vessel-like structures shows a greater average area and volume in the gels co-cultured with stromal cells (Figures 3B and C). As shown by quantification of the total cell numbers, this is a consequence of a four-fold difference in the amount of endothelial cells (Figure 3D). Stromal cells are significantly more near to the endothelial structures, although that closeness may relate to a lack of space due to the superlative endothelial size and not to a tight interaction between these cell types (Figure 3E). Overall, pericytes promote the organization of endothelial cells into capillary-like structures while stromal cells stimulate their amorphous proliferation.

In co-culture with ECs, the stromal cells seem to lose the elongated phenotype after the ten days of culture, a phenomenon that can not be found in the angiogenesis setup. A major subset of the stromal cells are the fibroblasts, a cell type highly specialized in matrix degradation and deposition (Viswanathan et al. 2019). In wound healing, fibroblasts release a great amount of proteases that degrade fibrin networks (Plikus et al. 2021). During the remodeling, especially in low-density hydrogels like the one used in this study, fibroblasts could temporarily lose their attaching points and become more rounded (Fisher et al. 2008; Tamariz and Grinnell 2002). However, a comparison of the supporting cell type morphology was performed based on average sphericity and oblate/prolate ellipticity and no significant difference could be found.

Quantification of the protein content in the cell media on the last day of culture reveals differences in the concentration of angiopoietin-2 (Ang-2), placental growth factor (PlGF), and interleukin-6 (IL-6). Ang-2 can be both a pro and anti-vasculogenic molecule since it acts increasing the activity of VEGF when it is present and inhibiting vessel development in its absence (Akwii et al. 2019). The extremely low concentration of free VEGF in the media suggests that in this case Ang-2 acts as a vasculogenesis inhibitor, concurring with the lack of proper tubular structures in the stromal cell co-culture. PlGF is a pro-angiogenic protein from the same family as vascular endothelial growth factor (VEGF) and platelet-derived growth factor (PDGF), and despite its name it is also expressed in the umbilical cord and adult tissues (Falco 2012). PlGF binds to VEGF receptor 1 (Flt-1/VEGFR1), freeing the VEGF that is captured by it. This allows the VEGF to bind to VEGF receptor 2 (KDR/VEGFR2), starting a strong pro-vasculogenesis signal in the endothelial cells (Peach et al. 2018). Its high concentration in the pericyte co-culture may relate to the improved vessel formation in that condition. Finally, IL-6 is a pro-

inflammatory interleukin released during wound healing processes and its receptor is highly expressed by pericytes. Its binding activates STAT3, increasing mural cell recruitment and the release of pro-vasculogenic growth factors (Didion 2017; Villar-Fincheira et al. 2021).

Overall, in our study, the endothelial structures formed in the presence of the stromal cells resemble the bloated and disorganized networks of the primitive plexus typical of the vasculogenesis processes that occur in the early embryo (Udan et al. 2013). In contrast, pericytes seem to inhibit this process and promote the formation of structures more similar to the vessels found in later stages of development. At the same time, pericytes seem to arrest the proliferative capacity of the endothelial cells, leading to a smaller final endothelial volume.

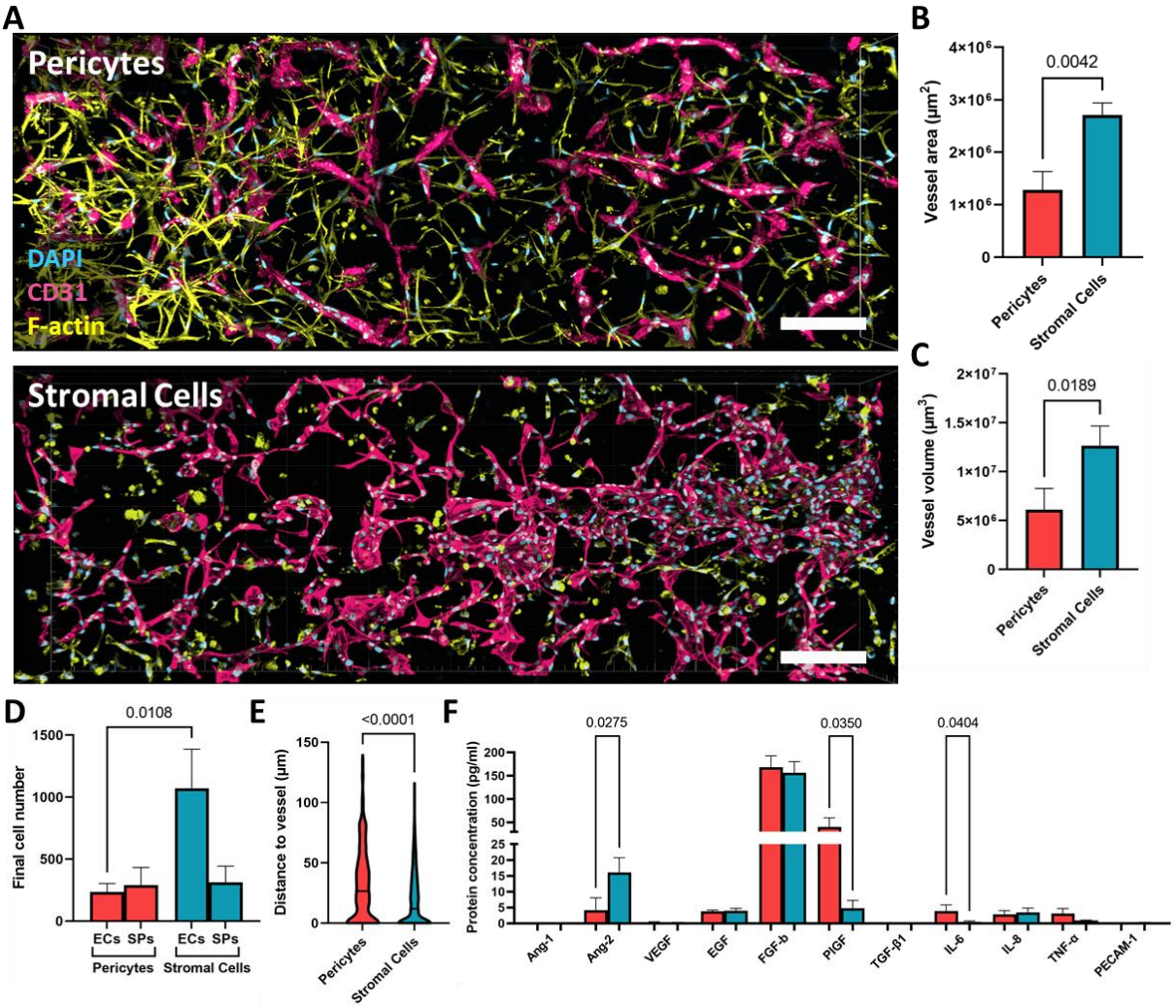

Figure 3. Comparison of pericytes and stromal cells in promoting vasculogenesis of endothelial cells.

(A) Immunofluorescence images of the vasculogenesis process within the microfluidic chips co-cultured with either pericytes or unselected ASCs, stained for nuclei (DAPI; cyan), CD31 showing the endothelial vessel-like structures (magenta) and the supporting cells' actin cytoskeleton (Phalloidin; yellow). Scale bars: 200 µm.

(B-C) Comparison of total vessel area and volume between both co-culture conditions (n = 3, t-test).

(D) Comparison of the final total number of endothelial cells (ECs) and supporting cells (SPs) in the two conditions (n = 3, t-test).

(E) Comparison of the distance between each type of supporting cell and the nearest vessel-like structure. The trunked violin plots depict summary statistics and the kernel density estimation to show the frequency distribution of each condition. The middle line represents the median (n = 3, Mann-Whitney test).

(F) Protein names: Angiopoietins 1 and 2 (Ang-1/-2), Vascular Endothelial Growth Factor (VEGF), Epidermal Growth Factor (EGF), Fibroblast Growth Factor-basic (FGF-b), Placental Growth Factor (PlGF), Tumor Growth Factor-beta 1 (TGF-β1) interleukins 6 and 8 (IL-6/-8), Tumor Necrosis Factor-alpha (TNF-α) and Platelet endothelial cell adhesion molecule (PECAM-1) (n = 3, t-test; corrected for multiple comparisons).

The main identifier of *in vivo* pericytes is the presence of a dense proteic fiber network shared with the endothelial vessels and enwrapping both of them, known as the basement membrane. Confirming the previous findings, transmission electron microscopy (TEM) reveals a close association of these pericytes with the endothelial vessels, with them forming a common basement membrane of shared matrix fibers (Figure 4). Such an interaction is rarely observed between the stromal cells and the ECs, which only present a loose association without a remarkable amount of shared fibers.

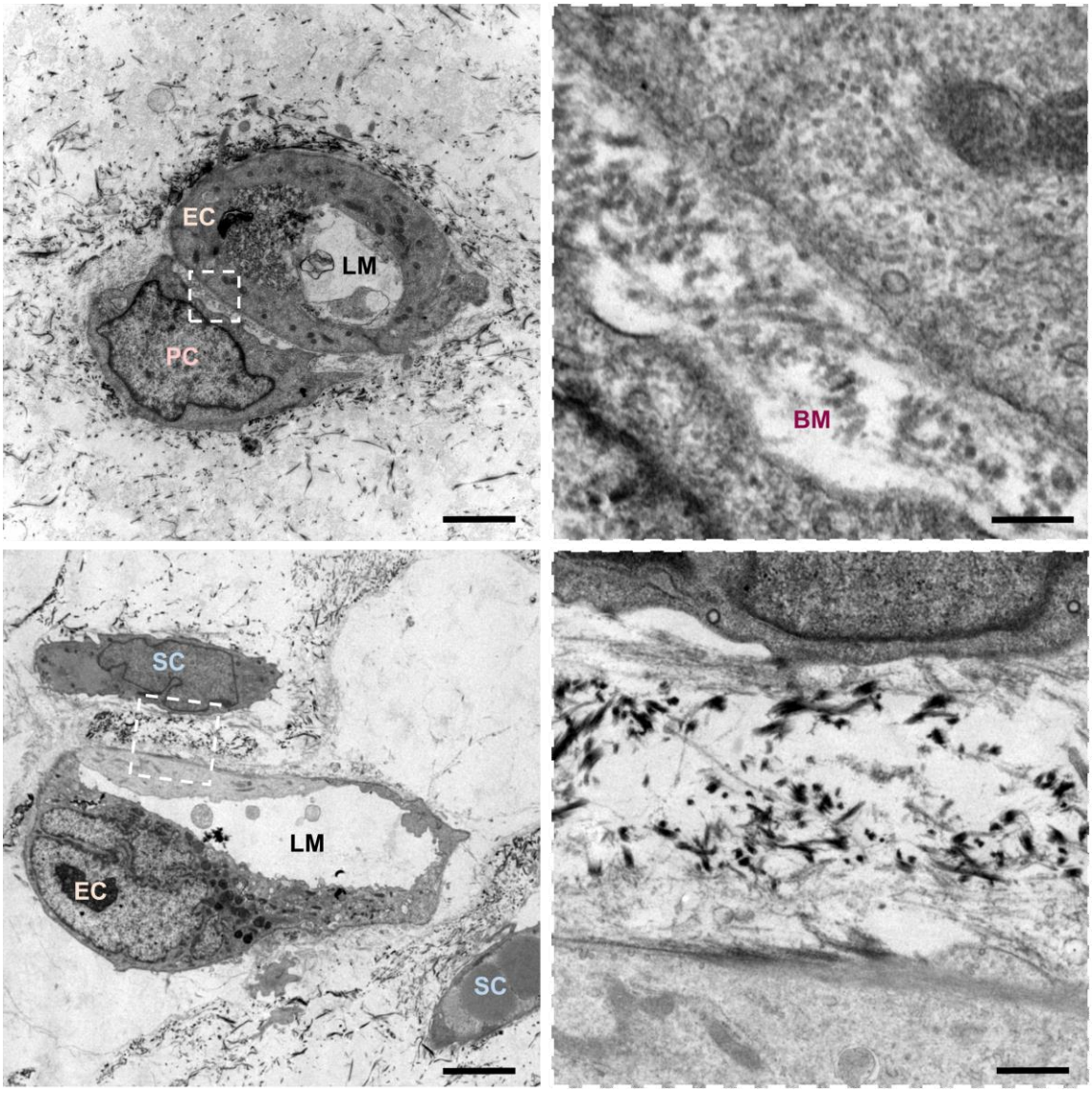

Figure 4. TEM image of the contact between the supporting cells and the vessels. Only pericytes possess a common basement membrane matrix with the endothelial cells. EC: Endothelial Cell; PC: Pericyte; SC: Stromal Cell; BM: Basement membrane; LM: Lumen. Scale bars: 2500 nm (top left), 5000 nm (bottom left), 250 nm (right).

We used RNA-seq to better understand the differences found in vasculogenesis in how pericytes and stromal cells differently regulate endothelial cell division and organization. Briefly, vasculogenesis co-

cultured gels incubated for ten days were minced and dissolved to isolate its RNA and perform bulk 3'mRNA-Seq. Heatmap and dendrogram show the 1550 significantly differently expressed genes (Signature genes) between both co-culture conditions (Adjusted p-value > 0.05; Figure 5A). These differently expressed genes are evenly distributed between both cell types (Figure 5B). To better visualize the most relevant results, the 200 signature genes of each co-culture condition with the highest fold change were plotted in a network showing the relations (edges) between genes (nodes), removing the genes with no known interaction (Figure 5C).

Gene set enrichment analysis (GSEA) of all signature genes shows that pericytes clearly promote the upregulation of genes related to blood vessel formation and organization (Figures D and E). No known signaling is exclusive of either adult angiogenesis or vasculogenesis, since both involve the activation of the same pathways (Patel-Hett and D'Amore 2011). Within them, Notch overexpression to the pericyte co-culture is central in the regulation of EC behavior during neovascularization (Fernández-Chacón et al. 2021). The detection of free VEGFA by the KDR/VEGFR2 receptor activates an EC as a “tip cell”, suppressing its proliferation and driving it to lead vessel elongation. Delta-like ligands (DLL4) on tip cells interact with Notch receptors (Notch1 and Notch4) on adjacent cells, inhibiting their tip cell behavior and marking them as “stalk cells” (Hellström et al. 2007). This process is crucial to control tubulogenesis and avoid aberrant networks.

Elaborating in other upregulated pathways in pericytes according to the Hallmark analysis, Sonic Hedgehog (SHH) coordinates both embryological and post-natal vascularization through both its canonical and non-canonical pathways, promoting EC survival, differentiation, and maturation (Salybekov et al. 2018). SHH upregulates Notch1 in both ECs and pericytes. The Wnt pathway, on the other hand, regulates vascularization through β-catenin-dependent mechanisms that affect cytoskeleton organization, directly affecting vessel tubulogenesis, remodeling, and stability (Olsen et al. 2017). The formation of vessel lumen is dependent on mitotic spindle orientation since it will establish the apical-basal polarity of the ECs (Wu et al. 2020). The apex of the lateral membrane of these adjacent polarized ECs is joined by apical junctions, which have a major role in regulating cell-cell adhesion and paracellular permeability (Rusu and Georgiou 2020; Wang and Margolis 2007).

The transforming growth factor beta (TGF-β) pathway regulates pericyte attraction and activity, and acts as a cytostatic by the inhibition of c-Myc expression, stabilizing new vessels (Guerrero and McCarty 2017). Both phosphoinositide 3-kinase/AKT/mammalian target of rapamycin (PI3K/AKT/mTOR) and Kirsten rat sarcoma virus (KRAS) are related pathways activated in ECs by pro-angiogenic molecules and act regulating the secretion of VEGF, nitric oxide and Ang1/2 (Mendoza et al. 2011).

As previously shown, free IL-6 was significantly more present in the pericyte co-culture media after the last 24 hours of incubation. The mRNA analysis shows the IL-6 upregulation in pericytes with respect to stromal cells, together with many other pro-inflammatory cytokines. Tumor necrosis factor alpha (TNFa), interferon alpha and gamma, and the NF-kB signaling pathways are all downregulated in stromal cells. Stromal cells are widely known to have immunomodulatory properties which are being explored in cell therapy (Caplan 2017; Melief et al. 2013; Viswanathan et al. 2019; Bourin et al. 2013; Galderisi et al. 2022). That is in line with the downregulation of many inflammatory molecules observed in that co-culture condition (Patrikoski et al. 2019).

The GO Cellular Component analysis reveals overexpression of cell-cell and cell-matrix junctions in the pericyte co-cultures, such as Claudin 5 (CLD5) and many types of integrins (ITGA) (Mongiat et al. 2016; Dejana and Orsenigo 2013). The tightness of the endothelium barrier is dependent on these cellular connections, essential to maintain the structural integrity of the vessels and avoid the leakage of the blood contents. Some of the upregulated integrins are also directly involved in vasculogenesis such as ITGA1 or 11 (Mongiat et al. 2016).

Stromal cell co-culture shows a robust upregulation of Myc targets and hypoxia pathways, both profoundly involved in cell proliferation (Bretones et al. 2015; Kaluz et al. 2008; Batie et al. 2019; Pugh and Ratcliffe 2003). Another pro-mitotic signaling such as p53 and G protein cascades are also upregulated (Carlton et al. 2020; Engeland 2022). The consequences are shown by the increased cytoplasmic translation and ribosomal, mitochondrial, and nucleolar biogenesis, intrinsic parts of cell division (Carlton et al. 2020). The increased DNA repair mechanisms and oxidative phosporylation may indicate a response to the increased metabolic activity and replication stress associated with cell proliferation (Saxena and Zou 2022; Magdalou et al. 2014). Stromal cells also overexpress genes involved in collagen genesis and deposition, explained by the large percentage of fibroblasts present in this population (Sun et al. 2019).

Not all differences in gene expression can be translated to protein amount and signaling, since mRNAseq is blind to post-transcriptional regulation and protein stability and degradation. However, there is a very clear trend of upregulated vasculogenesis and tubulogenesis genes in the co-cultures supported by pericytes, including Notch, TGF-β, IL-6, SHH, and Wnt. On the other hand, stromal cells lead to the overexpression of genes related to cell division and organelle biogenesis (such as Myc and p53), together with the associated cell stress and accelerated metabolism; and the downregulation of inflammatory cytokines that characterize this population. This is fitting all the previously shown results (Figures 3 and 4).

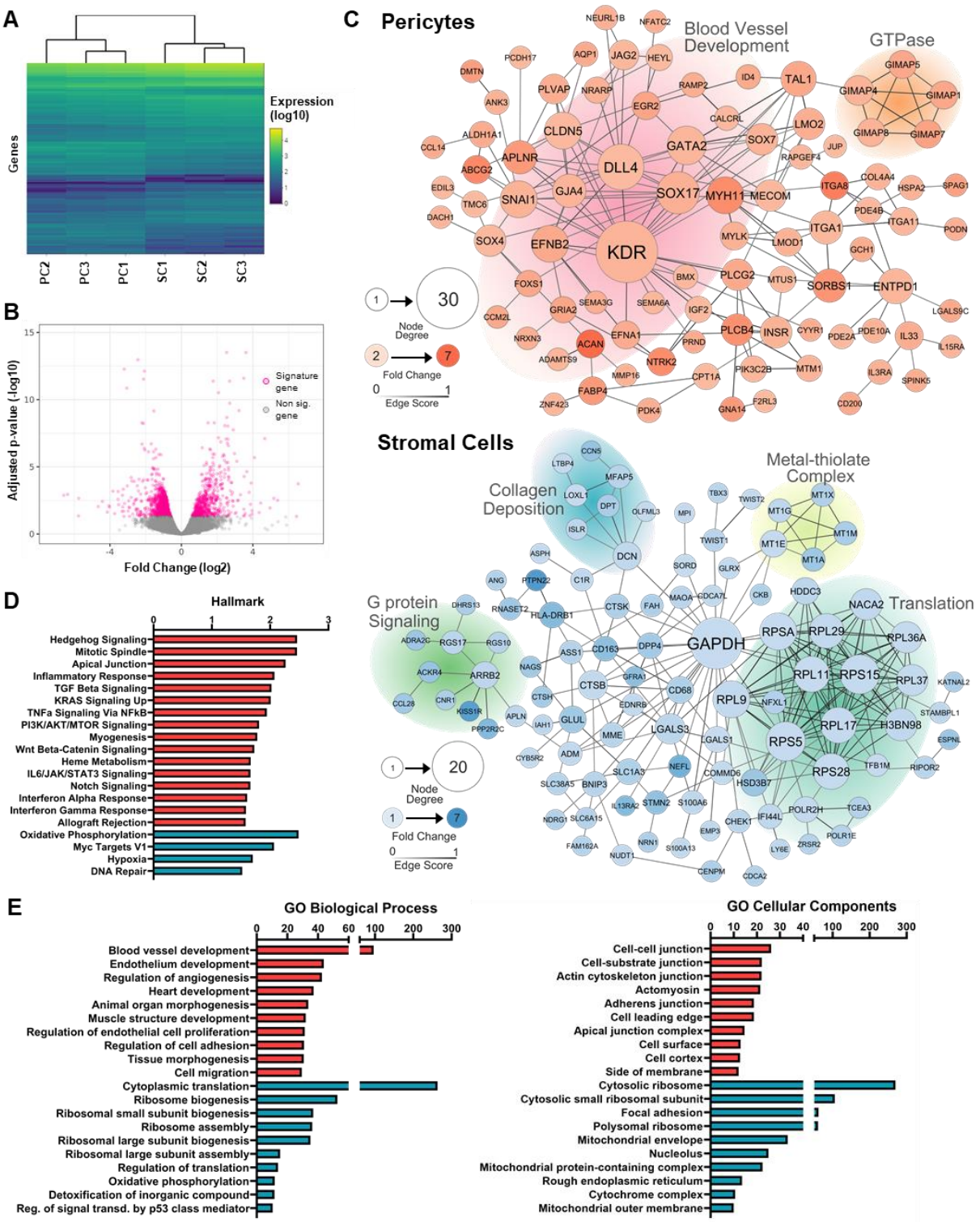

Figure 5. Gene expression analysis of pericyte and stromal cell co-cultures with ECs

(A) Dendrogram and heat map of hierarchical clustering of the 1550 differently expressed genes between the three pericyte (PC) and stromal cell (SC) donors.

(B) Volcano plot of the 1550 differently expressed genes plotting their fold change (log2) by adjusted p-value (-log10). Positive fold change values are signature genes in pericytes, while negative ones are in the stromal cells.

(C) Network visualization of the top differently expressed genes in both types of co-cultures. Each node represents a signature gene and the connections to other genes show a known relation in their expressions. The node color visualizes the fold change of its expression, and the size represents its importance in the network,

understood as the number of relations with other genes. The tone of the connections shows the "Edge score", the strength of the relation between them. The background-shading groups are merely orientative and represent relevant gene sets based on the GO databases.

(D) Hallmark gene sets from MsigDB on the differentially expressed genes between pericytes (red) and stromal cell (blue) co-cultures. The scale bar represents the Normalized Enrichment Score (NES).

(E) Ontological analysis of the differently expressed genes based on GO databases, of pericytes (red) and stromal cells (blue). The scale bar represents the adjusted False Discovery Ratio (FDR).

Conclusions

The relationship between pericytes and mesenchymal stromal/stem cells has been widely debated in the last years, ranging from considering them as two completely independent populations to suggesting the latter as an activated form of the pericyte (Blocki et al. 2013; Souza et al. 2016; Blocki et al. 2018; Guimarães-Camboa et al. 2017). It has also been discussed if the pericytic identity can be maintained in culture or if subsequent passages growing outside of the body would lead to a loss of its characteristics (Blocki et al. 2013). Here, we demonstrate that the isolation of pericytes from the stromal vascular fraction of the adipose tissue based on the expression of the MCAM marker provides a population of plastic-adherent cells that conserve their ability to act as a mural cell *in vitro* for at least five passages. Both immunofluorescence and TEM imaging proved this interaction. We also demonstrate that these pericytes act significantly differently from their unselected counterpart, promoting bigger and more branched sproutings in angiogenesis. In vasculogenesis, pericytes arrest endothelial cell division and stimulate their arrangement in vessel-like structures. Stromal cells, on the other hand, stimulate endothelial cell proliferation, forming aggregates similar to the primitive capillary plexus. These results are relevant both to understand the function of pericytes *in vitro* and to improve current strategies for *in vitro* vascularization. For instance, the propensity of stromal cells to induce endothelial proliferation could be harnessed to support the first steps of vasculogenesis, while the vessel-stabilizing influence of pericytes might be critical in preventing pathological vascularization.

Experimental Section

Cell isolation and culture

ASCs and pericytes were isolated from adipose tissue kindly provided by the Clinic for Plastic, Hand and Burns Surgery (University Hospital Aachen). First, the adipose layer was separated from the dermis and manually minced until achieving a homogenous slurry. The minced fat was added to gentleMACS C-Tubes (Miltenyi), mixed with the same volume of collagenase I (1 mg/mL; Sigma-Aldrich), and placed in a gentleMACS Octo Dissociator to achieve complete homogeneization and digestion at 37ºC with consecutive stirring steps for 15 minutes. The mixture is left for another 30 minutes at 37ºC in soft agitation on a roller mixer. The digested SVF is then filtered using a 100 µm cell strainer (Falcon), mixed with sterile PBS, and centrifuged at 300 g. The supernatant is removed and the pellet is re-suspended in PBS for two more washing steps. To expand the stromal cells, one-quarter of the SVF suspension is seeded in a cell culture-plastic flask and cultured in Mesenpan media (PAN-Biotech) supplemented with 2% (v/v) fetal bovine serum (FBS; Gibco) and 1% (v/v) antibiotic/antimycotic solution (ABM; Gibco).

The other part of the SVF is diluted 1:10 in Erythrocyte Lysis Buffer (PAN-Biotech), briefly vortexed, and incubated at room temperature (RT) for 10 minutes. The mixture is washed another 3 times as previously described. The resulting pellet is resuspended in 10 µL anti-CD146 magnetic microbeads

(Miltenyi) and 90 µL blocking buffer (Miltenyi), and incubated for 15 minutes at 4°C. The mixture is washed again three times to remove unattached magnetic microbeads. A MACS LS column (Miltenyi) is attached to a magnetic separator (Miltenyi) and prepared by rinsing it with PBS. The labeled cell suspension is added to the column and rinsed three times with Mesenpan to remove the CD146- cells. The column is then separated from the magnetic holder, filled with media, and pressed with a sterile plunger. The resulting CD146+ cell suspension is considered as pericytes and will be cultured as previously described in the same conditions as the ASCs.

Human umbilical vein endothelial cells (HUVECs) were isolated from human umbilical cords using collagenase type I (Sigma-Aldrich, 400 U/mL) to separate the cell layer surrounding the vein lumen. The detached cells were subsequently expanded in endothelial cell growth medium 2 (EGM2; Promocell) supplemented with 1% (v/v) ABM. The human umbilical cords were generously provided by the Clinic for Gynecology and Obstetrics at RWTH Aachen University Hospital and were used within 24 hours after delivery.

HUVECs, stromal cells, and pericytes were cryopreserved in liquid nitrogen using a freezing solution consisting of 60% (v/v) DMEM, 20% (v/v) FBS, and 20% (v/v) DMSO. Prior to the device experiment, HUVECs were thawed and expanded up to passage 3 in EGM2. Stromal cells and pericytes were cultured up to passage 4 in Mesenpan.

Preparation of the vascularization assays in microfluidic devices

HUVECs, stromal cells, and pericytes were detached by trypsin/EDTA (Pan-Biotech) digestion. Cells were then suspended in tris-buffered saline (TBS) solution containing thrombin (Sigma-Aldrich) and calcium chloride (CaCl2; Sigma-Aldrich). This mixture was combined with a fibrinogen solution (VWR) pre-cooled on ice and either 10 µL were injected into the central chamber of the idenTx 3 microfluidic chip (AIM Biotech) for the chip experiments or 350 µL were directly deposited into 24-well plate wells for the bulk gels. The resulting gel contained 5 mg/mL fibrinogen, 3 IU/mL thrombin and 3.75 mM $CaCl_2$ dissolved in 50 µg/mL TBS.

For imaging after the preparation, cells were pre-stained with Vybrant dyes (Invitrogen) by adding 5 µL of cell-labeling solution to a 1 x 10^6 cell/mL cell suspension in serum-free cell media. The mixture was vortex and incubated for 20 minutes at 37°C. Then, cells were centrifuged at 300 g and washed with PBS three times to remove residual dye.

For the vasculogenesis chip set-up, 10 x 10^6 HUVECs/mL and 2 x 10^6 supporting cells/mL were pre-mixed in the injected solution. For the bulk vasculogenesis gel, 10 x 10^6 HUVECs/mL and 5 x 10^6 supporting cells/mL were added. For the angiogenesis chip set-up, only the supporting cells were suspended in the polymerizing solution. In all cases, the fibrin gels were incubated for 20 min at room temperature and another 20 min at 37°C and 5% CO2 in a humidified atmosphere to achieve the complete polymerization of the fibrin. For the angiogenesis assay, the bottom channel was filled with a solution of 50 µg/mL fibronectin in EGM microvascular vessel 2 (EGM-MV 2, PromoCell) immediately after the polymerization and incubated for 40 minutes at 37°C. The fibronectin was washed away with EGM-MV 2 and a solution of 2 x 10^5 HUVECs/mL was injected in the coated channel.

Chips of both set-ups were filled with EGM-MV 2 supplemented with 1% (v/v) ABM, adding 100 µL to the bottom left well, 80 µL to the bottom right well, 60 µL to the top left well and 40 µL to the top right well, to achieve gravity-driven flow both inside each of the channels and between them through the hydrogel chamber. The chips were placed in humidified chambers with the bottom exposed to air, in a 5% CO2 and 37°C atmosphere. The media was changed every 24 hours for 10 days. For the bulk gels in 24-well plates, 500 µL of EGM-MV 2 was added and changed every 48-72 hours. Three biological replicates (independent donors) were used.

For fixation, the medium was removed from the channels and substituted with ice-cold methanol at -20°C. All fibrin gels were incubated at 4°C for 30 minutes and then washed three times with PBS.

Immunofluorescence imaging

The fixed chips were first stained with mouse anti-CD31 (PECAM-1, 1:100; Sigma-Aldrich) solved in antibody diluent made of 3% Bovine Serum Albumin (BSA) and 1% ABM for 48 hours at 37°C. Then, the samples were washed three times. Afterward, a mixture of Alexa Fluor® 594 goat anti-mouse IgG (1:400, Invitrogen) and Phalloidin-iFluor™ 488 Conjugate (Cayman Chemical) was added to the samples and incubated for 48 hours at 37°C. The chips were washed, stained with 0.4 µg/mL of a DAPI solution for 2 hours at 37°C, washed again, and stored at 4°C until imaging. Microscopy was done with a LSM 980 with Airyscan 2 (Zeiss) confocal laser scanning microscope, creating stacks of the whole gel thickness, 200 µm, with a step size of 3 µm. The resulting composite was processed with Imaris 10 (Oxford Instruments), creating 3D surfaces of the CD31+ vessel-like objects. The volume of these objects was measured. Only in the case of the angiogenesis model, the structures were considered tubular and homogenous enough to assess them as cylinders, to approximate the diameter based on the area and volume data. The number of branching and sprouting points was manually counted. The vessel-like objects were subtracted from the F-actin channel to show only the supporting cells. From this, 3D surfaces were again created to measure the distance of these cells from the CD31+ structures.

The data was analyzed for normality with the Shapiro-Wilk test. Except for the “distance to vessel” data of the angiogenesis assay, all results were normally distributed and unpaired t-test were performed. For the “distance to vessel” data, a non-parametric Mann-Whitney Test was used.

TEM imaging

The bulk fibrin gels were fixed in a 3% glutaraldehyde solution for at least 24 hours. They were then rinsed in 0.1 M Soerensen’s phosphate buffer (Merck) and fixed with 1% osmium tetraoxide (Carol Roth) in a 17% sucrose buffer (Merck). After a dehydration process with a series of increasing ethanol concentrations, the samples were immersed in propylene oxide, then in a 1:1 mixture of Epon resin (Serva) and propylene oxide for one hour, followed by a final one-hour incubation in pure Epon resin. The samples were then embedded in pure Epon at 90 °C for two hours.

Ultrathin sections between 70 to 100 nm were obtained using an ultramicrotome (Reichert Ultracut S, Leica) equipped with a Diatome diamond knife. These sections were placed onto Cu/Rh grids (HR23 Maxtaform, Plano). To enhance contrast, the sections were stained with a 0.5% uranyl acetate and 1% lead citrate solution (both from EMS). The final observation was performed using a Zeiss Leo 906 (Carl Zeiss) transmission electron microscope, operated at an acceleration voltage of 60 kV.

RNA isolation, sequencing and analysis

RNA isolation was performed using TRIzol (Invitrogen) and following the manufacturer‘s user guide. Briefly, cold TRIzol was added to the fibrin gel and incubated for 5 minutes. The mixture was then pipetted up and down until the gel disagreggates, and stored at -20ºC until isolation. After thawing, chloroform was added to the sample, incubated for 3 minutes, and centrifuged for 15 minutes at 12,000 g at 4ºC to separate the phases. The top aqueous phase containing the RNA was carefully extracted and placed in a different tube. Then, isopropanol was added and the tubes were centrifuged again to precipitate the RNA. The supernatant was discarded, RNA pellet was resuspended in 75% ethanol and centrifuged again. This process was repeated three times to remove isopropanol leftovers from the mixture. Finally, the RNA pellet was air-dried until no ethanol was left and resuspended in RNase-free water.

3'mRNA-Seq libraries were prepared using Lexogen QuantSeq 3'mRNA-Seq v2 Library Prep Kit FWD with UDIs following the manufacturer's protocol. Prior to library preparation, the concentration of RNA was measured using the Promega Quantus Fluorometer. Additionally, the size distribution of the RNA was assessed using the Agilent TapeStation with an RNA ScreenTape. Quantification and quality assessment were repeated after library preparation, again using the Quantus fluorometer and the Agilent TapeStation with a High Sensitivity D1000 ScreenTape. Libraries were denatured, diluted, and loaded onto a NextSeq High Output v2.5 (75 cycles) flow cell. The 1% PhiX control library was spiked in to improve base calling accuracy. Single-end sequencing was performed with 75 cycles on the Illumina NextSeq platform according to the manufacturer's instructions.

FASTQ files were generated using bcl2fastq (Illumina). To facilitate reproducible analysis, samples were processed using the publicly available nf-core/RNA-seq pipeline version 3.12 (Ewels et al. 2020) implemented in Nextflow 23.10.0 (Di Tommaso et al. 2017) with minimal command. In brief, lane-level reads were trimmed using Trim Galore 0.6.7 (Felix Krueger et al. 2023) and aligned to the human genome (GRCh39) using STAR 2.7.9a (Dobin et al. 2013). Gene-level and transcript-level quantification was done by Salmon v1.10.1 (Patro et al. 2017). Heatmap/dendrogram and volcano plot visualizations were performed using custom scripts in R version 4.3.2 using the DESeq2 v.1.32.0 framework (Love et al. 2014).

For the hallmark gene set analysis, Gene Set Enrichment Analysis (GSEA) was performed using clusterProfiler version 4.6.2. Pre-ranked gene lists, generated from differential gene expression analysis, were input into clusterProfiler to identify enriched biological pathways (Liberzon et al. 2015). Enriched hallmark gene sets with an FDR q-value < 0.05 were considered significant.

Gene network visualization and functional enrichment of GO pathways were done using the stringApp v2.0.3 (Doncheva et al. 2019) of CytoScape 3.10.1 (Shannon et al. 2003). For the gene networks, the top 200 genes with higher adjusted p-values of each co-culture type were plotted using the STRING visualization. Singletons and pairs were removed, and the remaining network was organized with the Prefuse Force Directed Layout. Then, enrichment data for all the signature genes of GO Biological Processes and GO Cellular Components was exported with a redundancy cutoff of “0.7” to remove nearly identical terms. The ten pathways with the highest adjusted FDR of each condition were plotted using GraphPad Prism 9.5.1.

Acknowledgements

Human tissues were obtained following the Declaration of Helsinki after informed at RWTH Aachen University Hospital, Aachen, Germany. Umbilical cords were provided by the Centralized Biomaterial Bank of the RWTH Aachen University (cBMB) according to its regulations, following RWTH Aachen University, Medical Faculty Ethics Committee (cBMB project number 323) and the Department of Gynecology and Perinatal Medicine (Univ.-Prof. Dr. Stickeler). We wish to express our gratitude to the Clinic for Plastic, Hand and Burns Surgery (Univ.-Prof. Dr. Beier) for providing fat tissue (University Hospital Aachen, RWTH University Aachen, Germany, ethics approval reference number EK197-19). Figure 1A and B were created with BioRender. This work was supported by the Confocal Microscopy Facility and the Genomics Facility of the Interdisciplinary Center for Clinical Research (IZKF) Aachen within the Faculty of Medicine at RWTH Aachen University.

This study was funded by the Deutsche Forschungsgemeinschaft (DFG) (grant number 496706372) and the German Federal Ministry of Education and Research (Grant number 031B1150B(X)).

Publication bibliography

Akwii, Racheal G.; Sajib, Md S.; Zahra, Fatema T.; Mikelis, Constantinos M. (2019): Role of Angiopoietin-2 in Vascular Physiology and Pathophysiology. In *Cells* 8 (5). DOI: 10.3390/cells8050471.

Alimperti, Stella; Mirabella, Teodelinda; Bajaj, Varnica; Polacheck, William; Pirone, Dana M.; Duffield, Jeremy et al. (2017): Three-dimensional biomimetic vascular model reveals a RhoA, Rac1, and N-cadherin balance in mural cell-endothelial cell-regulated barrier function. In *Proceedings of the National Academy of Sciences of the United States of America* 114 (33), pp. 8758–8763. DOI: 10.1073/pnas.1618333114.

Batie, Michael; Frost, Julianty; Frost, Mark; Wilson, James W.; Schofield, Pieta; Rocha, Sonia (2019): Hypoxia induces rapid changes to histone methylation and reprograms chromatin. In *Science (New York, N.Y.)* 363 (6432), pp. 1222–1226. DOI: 10.1126/science.aau5870.

Blocki, Anna; Beyer, Sebastian; Jung, Friedrich; Raghunath, Michael (2018): The controversial origin of pericytes during angiogenesis - Implications for cell-based therapeutic angiogenesis and cell-based therapies. In *Clinical hemorheology and microcirculation* 69 (1-2), pp. 215–232. DOI: 10.3233/CH-189132.

Blocki, Anna; Wang, Yingting; Koch, Maria; Peh, Priscilla; Beyer, Sebastian; Law, Ping et al. (2013): Not all MSCs can act as pericytes: functional in vitro assays to distinguish pericytes from other mesenchymal stem cells in angiogenesis. In *Stem cells and development* 22 (17), pp. 2347–2355. DOI: 10.1089/scd.2012.0415.

Bourin, Philippe; Bunnell, Bruce A.; Casteilla, Louis; Dominici, Massimo; Katz, Adam J.; March, Keith L. et al. (2013): Stromal cells from the adipose tissue-derived stromal vascular fraction and culture expanded adipose tissue-derived stromal/stem cells: a joint statement of the International Federation for Adipose Therapeutics and Science (IFATS) and the International Society for Cellular Therapy (ISCT). In *Cytotherapy* 15 (6), pp. 641–648. DOI: 10.1016/j.jcyt.2013.02.006.

Bretones, Gabriel; Delgado, M. Dolores; León, Javier (2015): Myc and cell cycle control. In *Biochimica et biophysica acta* 1849 (5), pp. 506–516. DOI: 10.1016/j.bbagrm.2014.03.013.

Brooks, Anna E. S.; Iminitoff, Megan; Williams, Eloise; Damani, Tanvi; Jackson-Patel, Victoria; Fan, Vicky et al. (2019): Ex Vivo Human Adipose Tissue Derived Mesenchymal Stromal Cells (ASC) Are a Heterogeneous Population That Demonstrate Rapid Culture-Induced Changes. In *Frontiers in pharmacology* 10, p. 1695. DOI: 10.3389/fphar.2019.01695.

Caplan, Arnold I. (2017): Mesenchymal Stem Cells: Time to Change the Name! In *Stem cells translational medicine* 6 (6), pp. 1445–1451. DOI: 10.1002/sctm.17-0051.

Caporali, A.; Martello, A.; Miscianinov, V.; Maselli, D.; Vono, R.; Spinetti, G. (2017): Contribution of pericyte paracrine regulation of the endothelium to angiogenesis. In *Pharmacology & Therapeutics* 171, pp. 56–64. DOI: 10.1016/j.pharmthera.2016.10.001.

Carlton, Jeremy G.; Jones, Hannah; Eggert, Ulrike S. (2020): Membrane and organelle dynamics during cell division. In *Nat Rev Mol Cell Biol* 21 (3), pp. 151–166. DOI: 10.1038/s41580-019-0208-1.

Chandra, Prafulla; Atala, Anthony (2019): Engineering blood vessels and vascularized tissues: technology trends and potential clinical applications. In *Clinical science (London, England : 1979)* 133 (9), pp. 1115–1135. DOI: 10.1042/CS20180155.

Dejana, Elisabetta; Orsenigo, Fabrizio (2013): Endothelial adherens junctions at a glance. In *J Cell Sci* 126 (Pt 12), pp. 2545–2549. DOI: 10.1242/jcs.124529.

Di Tommaso, Paolo; Chatzou, Maria; Floden, Evan W.; Barja, Pablo Prieto; Palumbo, Emilio; Notredame, Cedric (2017): Nextflow enables reproducible computational workflows. In *Nat Biotechnol* 35 (4), pp. 316–319. DOI: 10.1038/nbt.3820.

Didion, Sean P. (2017): Cellular and Oxidative Mechanisms Associated with Interleukin-6 Signaling in the Vasculature. In *International journal of molecular sciences* 18 (12). DOI: 10.3390/ijms18122563.

Dobin, Alexander; Davis, Carrie A.; Schlesinger, Felix; Drenkow, Jorg; Zaleski, Chris; Jha, Sonali et al. (2013): STAR: ultrafast universal RNA-seq aligner. In *Bioinformatics* 29 (1), pp. 15–21. DOI: 10.1093/bioinformatics/bts635.

Doncheva, Nadezhda T.; Morris, John H.; Gorodkin, Jan; Jensen, Lars J. (2019): Cytoscape StringApp: Network Analysis and Visualization of Proteomics Data. In *Journal of proteome research* 18 (2), pp. 623–632. DOI: 10.1021/acs.jproteome.8b00702.

Engeland, Kurt (2022): Cell cycle regulation: p53-p21-RB signaling. In *Cell Death Differ* 29 (5), pp. 946–960. DOI: 10.1038/s41418-022-00988-z.

Ewels, Philip A.; Peltzer, Alexander; Fillinger, Sven; Patel, Harshil; Alneberg, Johannes; Wilm, Andreas et al. (2020): The nf-core framework for community-curated bioinformatics pipelines. In *Nat Biotechnol* 38 (3), pp. 276–278. DOI: 10.1038/s41587-020-0439-x.

Falco, Sandro de (2012): The discovery of placenta growth factor and its biological activity. In *Experimental & Molecular Medicine* 44 (1), pp. 1–9. DOI: 10.3858/emm.2012.44.1.025.

Felix Krueger; Frankie James; Phil Ewels; Ebrahim Afyounian; Michael Weinstein; Benjamin Schuster-Boeckler et al. (2023): FelixKrueger/TrimGalore: v0.6.10 - add default decompression path: Zenodo. Available online at https://zenodo.org/records/7598955.

Fernández-Chacón, Macarena; García-González, Irene; Mühleder, Severin; Benedito, Rui (2021): Role of Notch in endothelial biology. In *Angiogenesis* 24 (2), pp. 237–250. DOI: 10.1007/s10456-021-09793-7.

Fisher, Gary J.; Varani, James; Voorhees, John J. (2008): Looking older: fibroblast collapse and therapeutic implications. In *Arch Dermatol* 144 (5), pp. 666–672. DOI: 10.1001/archderm.144.5.666.

Galderisi, Umberto; Peluso, Gianfranco; Di Bernardo, Giovanni (2022): Clinical Trials Based on Mesenchymal Stromal Cells are Exponentially Increasing: Where are We in Recent Years? In *Stem Cell Rev and Rep* 18 (1), pp. 23–36. DOI: 10.1007/s12015-021-10231-w.

Guerrero, Paola A.; McCarty, Joseph H. (2017): TGF-β Activation and Signaling in Angiogenesis. In : Physiologic and Pathologic Angiogenesis - Signaling Mechanisms and Targeted Therapy: InTech.

Guimarães-Camboa, Nuno; Cattaneo, Paola; Sun, Yunfu; Moore-Morris, Thomas; Gu, Yusu; Dalton, Nancy D. et al. (2017): Pericytes of Multiple Organs Do Not Behave as Mesenchymal Stem Cells In Vivo. In *Cell stem cell* 20 (3), 345-359.e5. DOI: 10.1016/j.stem.2016.12.006.

Hellström, Mats; Phng, Li-Kun; Hofmann, Jennifer J.; Wallgard, Elisabet; Coultas, Leigh; Lindblom, Per et al. (2007): Dll4 signalling through Notch1 regulates formation of tip cells during angiogenesis. In *Nature* 445 (7129), pp. 776–780. DOI: 10.1038/nature05571.

Kaluz, Stefan; Kaluzová, Milota; Stanbridge, Eric J. (2008): Regulation of gene expression by hypoxia: integration of the HIF-transduced hypoxic signal at the hypoxia-responsive element. In *Clinica chimica acta; international journal of clinical chemistry* 395 (1-2), pp. 6–13. DOI: 10.1016/j.cca.2008.05.002.

Kosyakova, Natalia; Kao, Derek D.; Figetakis, Maria; López-Giráldez, Francesc; Spindler, Susann; Graham, Morven et al. (2020): Differential functional roles of fibroblasts and pericytes in the

formation of tissue-engineered microvascular networks in vitro. In *npj Regen Med* 5 (1), p. 1. DOI: 10.1038/s41536-019-0086-3.

Leung, Chak Ming; Haan, Pim de; Ronaldson-Bouchard, Kacey; Kim, Ge-Ah; Ko, Jihoon; Rho, Hoon Suk et al. (2022): A guide to the organ-on-a-chip. In *Nat Rev Methods Primers* 2 (1), pp. 1–29. DOI: 10.1038/s43586-022-00118-6.

Liberzon, Arthur; Birger, Chet; Thorvaldsdóttir, Helga; Ghandi, Mahmoud; Mesirov, Jill P.; Tamayo, Pablo (2015): The Molecular Signatures Database (MSigDB) hallmark gene set collection. In *Cell systems* 1 (6), pp. 417–425. DOI: 10.1016/j.cels.2015.12.004.

Love, Michael I.; Huber, Wolfgang; Anders, Simon (2014): Moderated estimation of fold change and dispersion for RNA-seq data with DESeq2. In *Genome Biol* 15 (12), p. 550. DOI: 10.1186/s13059-014-0550-8.

Magdalou, Indiana; Lopez, Bernard S.; Pasero, Philippe; Lambert, Sarah A. E. (2014): The causes of replication stress and their consequences on genome stability and cell fate. In *Seminars in Cell & Developmental Biology* 30, pp. 154–164. DOI: 10.1016/j.semcdb.2014.04.035.

Melief, Sara M.; Zwaginga, Jaap Jan; Fibbe, Willem E.; Roelofs, Helene (2013): Adipose tissue-derived multipotent stromal cells have a higher immunomodulatory capacity than their bone marrow-derived counterparts. In *Stem cells translational medicine* 2 (6), pp. 455–463. DOI: 10.5966/sctm.2012-0184.

Mendoza, Michelle C.; Er, E. Emrah; Blenis, John (2011): The Ras-ERK and PI3K-mTOR pathways: cross-talk and compensation. In *Trends in biochemical sciences* 36 (6), pp. 320–328. DOI: 10.1016/j.tibs.2011.03.006.

Mongiat, Maurizio; Andreuzzi, Eva; Tarticchio, Giulia; Paulitti, Alice (2016): Extracellular Matrix, a Hard Player in Angiogenesis. In *International journal of molecular sciences* 17 (11). DOI: 10.3390/ijms17111822.

Olsen, Jun Jun; Pohl, Sebastian Öther-Gee; Deshmukh, Abhijeet; Visweswaran, Malini; Ward, Natalie C.; Arfuso, Frank et al. (2017): The Role of Wnt Signalling in Angiogenesis. In *The Clinical biochemist. Reviews* 38 (3), pp. 131–142. Available online at https://www.ncbi.nlm.nih.gov/pmc/articles/PMC5759160/.

Patel-Hett, Sunita; D'Amore, Patricia A. (2011): Signal transduction in vasculogenesis and developmental angiogenesis. In *The International journal of developmental biology* 55 (4-5), pp. 353–363. DOI: 10.1387/ijdb.103213sp.

Patrikoski, Mimmi; Mannerström, Bettina; Miettinen, Susanna (2019): Perspectives for Clinical Translation of Adipose Stromal/Stem Cells. In *Stem Cells International* 2019, p. 5858247. DOI: 10.1155/2019/5858247.

Patro, Rob; Duggal, Geet; Love, Michael I.; Irizarry, Rafael A.; Kingsford, Carl (2017): Salmon provides fast and bias-aware quantification of transcript expression. In *Nat Methods* 14 (4), pp. 417–419. DOI: 10.1038/nmeth.4197.

Peach, Chloe J.; Mignone, Viviane W.; Arruda, Maria Augusta; Alcobia, Diana C.; Hill, Stephen J.; Kilpatrick, Laura E.; Woolard, Jeanette (2018): Molecular Pharmacology of VEGF-A Isoforms: Binding and Signalling at VEGFR2. In *International journal of molecular sciences* 19 (4). DOI: 10.3390/ijms19041264.

Plikus, Maksim V.; Wang, Xiaojie; Sinha, Sarthak; Forte, Elvira; Thompson, Sean M.; Herzog, Erica L. et al. (2021): Fibroblasts: Origins, definitions, and functions in health and disease. In *Cell* 184 (15), pp. 3852–3872. DOI: 10.1016/j.cell.2021.06.024.

Pugh, Christopher W.; Ratcliffe, Peter J. (2003): Regulation of angiogenesis by hypoxia: role of the HIF system. In *Nat Med* 9 (6), pp. 677–684. DOI: 10.1038/nm0603-677.

Rusu, Alexandra D.; Georgiou, Marios (2020): The multifarious regulation of the apical junctional complex. In *Open biology* 10 (2), p. 190278. DOI: 10.1098/rsob.190278.

Salybekov, Amankeldi A.; Salybekova, Ainur K.; Pola, Roberto; Asahara, Takayuki (2018): Sonic Hedgehog Signaling Pathway in Endothelial Progenitor Cell Biology for Vascular Medicine. In *International journal of molecular sciences* 19 (10), p. 3040. DOI: 10.3390/ijms19103040.

Saxena, Sneha; Zou, Lee (2022): Hallmarks of DNA replication stress. In *Molecular cell* 82 (12), pp. 2298–2314. DOI: 10.1016/j.molcel.2022.05.004.

Shannon, Paul; Markiel, Andrew; Ozier, Owen; Baliga, Nitin S.; Wang, Jonathan T.; Ramage, Daniel et al. (2003): Cytoscape: a software environment for integrated models of biomolecular interaction networks. In *Genome Research* 13 (11), pp. 2498–2504. DOI: 10.1101/gr.1239303.

Souza, Lucas Eduardo Botelho de; Malta, Tathiane Maistro; Kashima Haddad, Simone; Covas, Dimas Tadeu (2016): Mesenchymal Stem Cells and Pericytes: To What Extent Are They Related? In *Stem cells and development* 25 (24), pp. 1843–1852. DOI: 10.1089/scd.2016.0109.

Sun, Yuan; Chen, Song; Zhang, Xicheng; Pei, Ming (2019): Significance of Cellular Cross-Talk in Stromal Vascular Fraction of Adipose Tissue in Neovascularization. In *Arteriosclerosis, thrombosis, and vascular biology* 39 (6), pp. 1034–1044. DOI: 10.1161/ATVBAHA.119.312425.

Sweeney, Mark; Foldes, Gabor (2018): It Takes Two: Endothelial-Perivascular Cell Cross-Talk in Vascular Development and Disease. In *Front. Cardiovasc. Med.* 5, p. 154. DOI: 10.3389/fcvm.2018.00154.

Tamariz, Elisa; Grinnell, Frederick (2002): Modulation of fibroblast morphology and adhesion during collagen matrix remodeling. In *Molecular Biology of the Cell* 13 (11), pp. 3915–3929. DOI: 10.1091/mbc.E02-05-0291.

Todorova, Dilyana; Simoncini, Stéphanie; Lacroix, Romaric; Sabatier, Florence; Dignat-George, Françoise (2017): Extracellular Vesicles in Angiogenesis. In *Circulation research* 120 (10), pp. 1658–1673. DOI: 10.1161/CIRCRESAHA.117.309681.

Udan, Ryan S.; Culver, James C.; Dickinson, Mary E. (2013): Understanding vascular development. In *Wiley interdisciplinary reviews. Developmental biology* 2 (3), pp. 327–346. DOI: 10.1002/wdev.91.

Vila Cuenca, Marc; Cochrane, Amy; van den Hil, Francijna E.; Vries, Antoine A. F. de; Lesnik Oberstein, Saskia A. J.; Mummery, Christine L.; Orlova, Valeria V. (2021): Engineered 3D vessel-on-chip using hiPSC-derived endothelial- and vascular smooth muscle cells. In *Stem cell reports* 16 (9), pp. 2159–2168. DOI: 10.1016/j.stemcr.2021.08.003.

Villar-Fincheira, Paulina; Sanhueza-Olivares, Fernanda; Norambuena-Soto, Ignacio; Cancino-Arenas, Nicole; Hernandez-Vargas, Felipe; Troncoso, Rodrigo et al. (2021): Role of Interleukin-6 in Vascular Health and Disease. In *Front. Mol. Biosci.* 8, p. 641734. DOI: 10.3389/fmolb.2021.641734.

Viswanathan, S.; Shi, Y.; Galipeau, J.; Krampera, M.; Leblanc, K.; Martin, I. et al. (2019): Mesenchymal stem versus stromal cells: International Society for Cell & Gene Therapy (ISCT®) Mesenchymal Stromal Cell committee position statement on nomenclature. In *Cytotherapy* 21 (10), pp. 1019–1024. DOI: 10.1016/j.jcyt.2019.08.002.

Wang, Q.; Margolis, B. (2007): Apical junctional complexes and cell polarity. In *Kidney International* 72 (12), pp. 1448–1458. DOI: 10.1038/sj.ki.5002579.

Wang, Yiyun; Xu, Jiajia; Chang, Leslie; Meyers, Carolyn A.; Zhang, Lei; Broderick, Kristen et al. (2019): Relative contributions of adipose-resident CD146+ pericytes and CD34+ adventitial progenitor cells in bone tissue engineering. In *npj Regen Med* 4 (1), p. 1. DOI: 10.1038/s41536-018-0063-2.

Wang, Zhaoqing; Xu, Qingji; Zhang, Nengwei; Du, Xuemei; Xu, Guangzhong; Yan, Xiyun (2020): CD146, from a melanoma cell adhesion molecule to a signaling receptor. In *Sig Transduct Target Ther* 5 (1), p. 148. DOI: 10.1038/s41392-020-00259-8.

Wu, Xuemei; Zhou, Jun; Li, Dengwen (2020): Orientation of the Mitotic Spindle in Blood Vessel Development. In *Front. Cell Dev. Biol.* 8, p. 583325. DOI: 10.3389/fcell.2020.583325.

Yamazaki, Tomoko; Mukouyama, Yoh-Suke (2018): Tissue Specific Origin, Development, and Pathological Perspectives of Pericytes. In *Frontiers in cardiovascular medicine* 5, p. 78. DOI: 10.3389/fcvm.2018.00078.

Yang, Guang; Mahadik, Bhushan; Choi, Ji Young; Fisher, John P. (2020): Vascularization in tissue engineering: fundamentals and state-of-art. In *Prog. Biomed. Eng.* 2 (1), p. 12002. DOI: 10.1088/2516-1091/ab5637.

Zhang, Boyang; Radisic, Milica (2020): Organ-level vascularization: The Mars mission of bioengineering. In *The Journal of thoracic and cardiovascular surgery* 159 (5), pp. 2003–2007. DOI: 10.1016/j.jtcvs.2019.08.128.

Zhao, Huaning; Chappell, John C. (2019): Microvascular bioengineering: a focus on pericytes. In *J Biol Eng* 13 (1), p. 26. DOI: 10.1186/s13036-019-0158-3.